

# Effect of the Plasma-assisted Patterning of the Organic Layers on the Performance of Organic Light-emitting Diodes

Yongtaek Hong<sup>\*</sup>, Jihoon Yang, Jeonghun Kwak<sup>\*\*</sup>, and Changhee Lee<sup>\*</sup>

## Abstract

In this paper, a plasma-assisted patterning method for the organic layers of organic light-emitting diodes (OLEDs) and its effect on the OLED performances are reported. Oxygen plasma was used to etch the organic layers, using the top electrode consisting of lithium fluoride and aluminum as an etching mask. Although the current flow at low voltages increased for the etched OLEDs, there was no significant degradation of the OLED efficiency and lifetime in comparison with the conventional OLEDs. Therefore, this method can be used to reduce the ohmic voltage drop along the common top electrodes by connecting the top electrode with highly conductive bus lines after the common organic layers on the bus lines are etched by plasma. To further analyze the current increase at low voltages, the plasma patterning effect on the OLED performance was investigated by changing the device sizes, especially in one direction, and by changing the etching depth in the vertical direction of the device. It was found that the current flow increase at low voltages was not proportional to the device sizes, indicating that the current flow increase does not come from the leakage current along the etched sides. In the etching depth experiment, the current flow at low voltages did not increase when the etching process was stopped in the middle of the hole transport layer. This means that the current flow increase at low voltages is closely related to the modification of the hole injection layer, and thus, to the modification of the interface between the hole injection layer and the bottom electrode.

**Keywords:** AMOLED, Plasma patterning, IR drop

## 1. Introduction

The active-matrix organic light-emitting diode display (AMOLED) has been used of late for small to medium-sized commercial display applications, and in the near future, medium to large AMOLED televisions will be available in the market. Although the organic light-emitting diode (OLED) technology has many advantages, such as a wide viewing angle, wide color gamut, high contrast ratio, low power consumption, and ultraslim and ultralight display implementation, there are many important technical issues regarding large display applications, one of which

concerns the voltage drop along the common power line of AMOLED due to the relatively high resistance of the OLED pixel's common electrodes. This voltage drop will become a significant problem as it will cause brightness uniformity, especially for AMOLEDs with a top-emission OLED structure. To address this issue, additional highly conductive bus lines are typically formed and electrically contacted to the relatively resistive common electrodes [1]. Highly conductive metal grid lines based on silver or copper materials can be printed directly on the common electrodes [2]. Since the direct printing or fabrication of the bus lines can degrade the OLED performance, a laser-assisted drilling method has been proposed for use on the OLED layers, followed by the exposure of the contact area before the common-electrode deposition. When the top electrode is deposited, an electrical contact with highly conductive bus lines is formed [3]. In this case, however, since the OLED pixel deposition process must be interrupted to establish electrical contact between the common electrodes and the bus lines, the interface between the organic layers and the top electrode can be degraded. Therefore, the so-called

Manuscript Received September 10, 2009; Revised September 21, 2009; Accepted for publication September 25, 2009.

This work was accomplished with support from SSDIP (SNU-Samsung SDI Display Innovation Program) and a Korea Research Foundation grant funded by the Korean government (MOEHRD, Basic Research Promotion Fund) (Grant No. KRF-2008-331-D00216).

<sup>\*</sup>Member, KIDS; <sup>\*\*</sup>Student Member, KIDS

Corresponding author: Yongtaek Hong

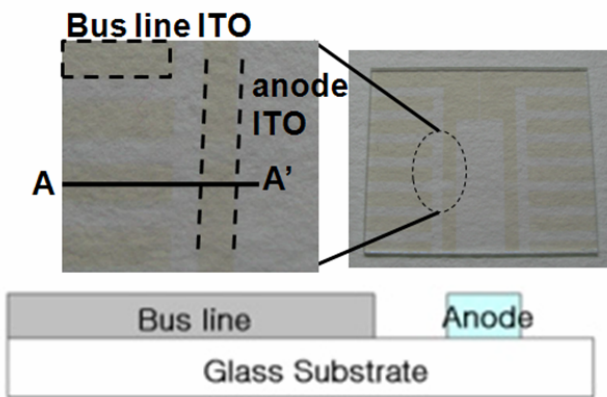
Department of Electrical Engineering and Computer Science, Seoul National University Inter-University Semiconductor Research Center, Seoul National University Kwanakro-599, Daehakdong, Kwanakgu, Seoul 151-744, Korea

E-mail: yongtaek@snu.ac.kr Tel: +82-2-880-9567 Fax: +82-2-872-9714

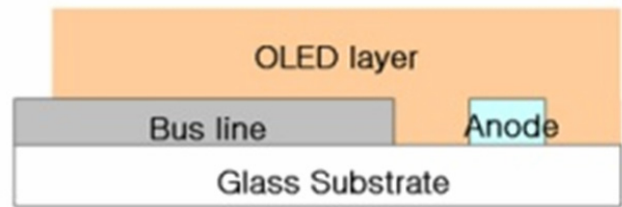
“double deposition method,” combined with the plasma-assisted etching of the OLED layer, was proposed so that the contact between the common electrode and the bus lines can be achieved without interruption during the OLED fabrication process [4].

Although the plasma-assisted patterning method has been widely used due to its fine physical etching characteristics and material selectivity in semiconductor fabrication

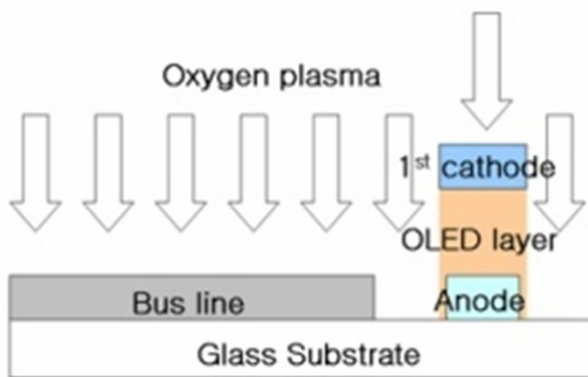
[5], it has not been used for OLED layer patterning because organic materials are believed to be damaged during the plasma etching process. Recently, however, the use of plasma-assisted patterning for active island patterning in organic thin-film transistor (OTFT) fabrication was reported [6-8]. An appropriate margin between the active region and the etched edge area must be taken into consideration. Otherwise, some degradation at the etched sides was also reported, leading to device performance degradation.



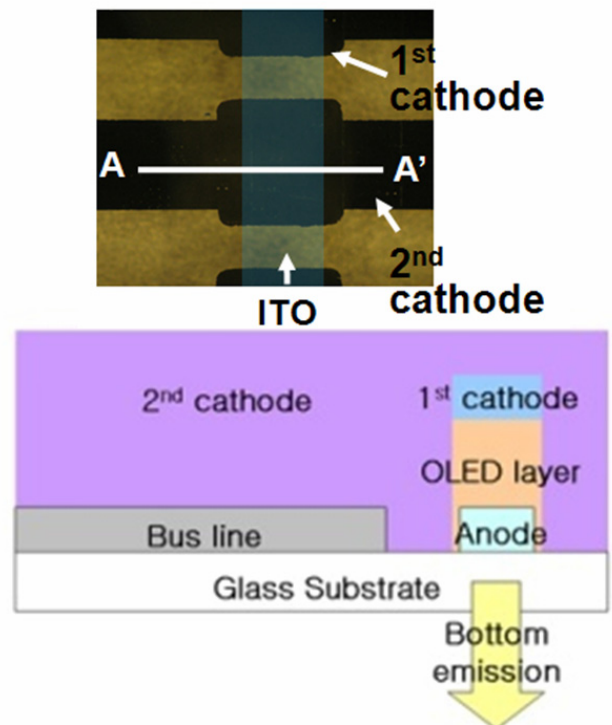
(a) ITO patterned substrate



(b) Flood coating of the organic layers



(c) First cathode deposition followed by plasma patterning



(d) Second cathode deposition

**Fig. 1.** OLED fabrication process.

Therefore, in this paper, the plasma patterning of the OLED layers and its effect on the device performance change is reported so that it can be used for voltage drop reduction without any significant performance degradation in AMOLED pixels.

## 2. Experiment

Fig. 2 shows a description of the fabrication process of the bottom-emission OLEDs that were used in this study. Top views of the indium-tin-oxide (ITO) patterned glass substrates and the fully fabricated OLED are also included, with cross-section-indicating lines (A-A') for the schematic cross-section figures. The substrates were cleaned in an ultrasonic bath of isopropyl alcohol, acetone, and methanol, and then dried in a vacuum oven. The cleaned ITO surface was treated in ultraviolet (UV) ozone for 5 min before organic-layer deposition. In this study, ITO was used as anode and bus lines for convenience (a). The thermal evaporation method was used for the deposition of the organic layers and cathode. The deposition process was done at the base pressure of  $2.1\sim 8.6\times 10^{-6}$  torr. The organic layers consist of three materials. We used 4,4',4"-tris (3-methylphenylphenylamino) triphenylamine (m-MTDATA) as the hole injection layer (HIL) material, 4,4'-bis [N-(1-naphthyl)-N-phenyl-amino] biphenyl (NPB) as the hole transport layer (HTL) material, and tris-(8-hydroxyquinoline) aluminum ( $\text{Alq}_3$ ) as the electron transport layer/electroluminescence layer (ETL/EML) material. The thicknesses of the layers were 15, 60, and 70 nm, respectively (b). Green-light emission (520 nm peak spectrum) was obtained from the fabricated OLEDs. 0.5-nm-thick lithium fluoride (LiF) was deposited as a buffer layer. The first cathode (aluminum) was deposited through a shadow mask. The thickness of the aluminum layer was varied to find the minimum thickness required for the oxygen plasma etch mask. Based on the preliminary results that were obtained, the aluminum thickness should be thicker than 20 nm for the etching equipment that was used. The area of the first cathode was larger than the actual emitting area ( $2\times 1.4\text{ mm}^2$ ) by 0.3 mm along one direction. After the fabrication, the samples were transferred in air to the oxygen plasma chamber. To compare the device performances, the other devices were also exposed to air for the time equivalent to the transfer process. The samples that were transferred to the oxygen plasma chamber were etched in 0.1-torr and 60-sccm  $\text{O}_2$  gas flow, with

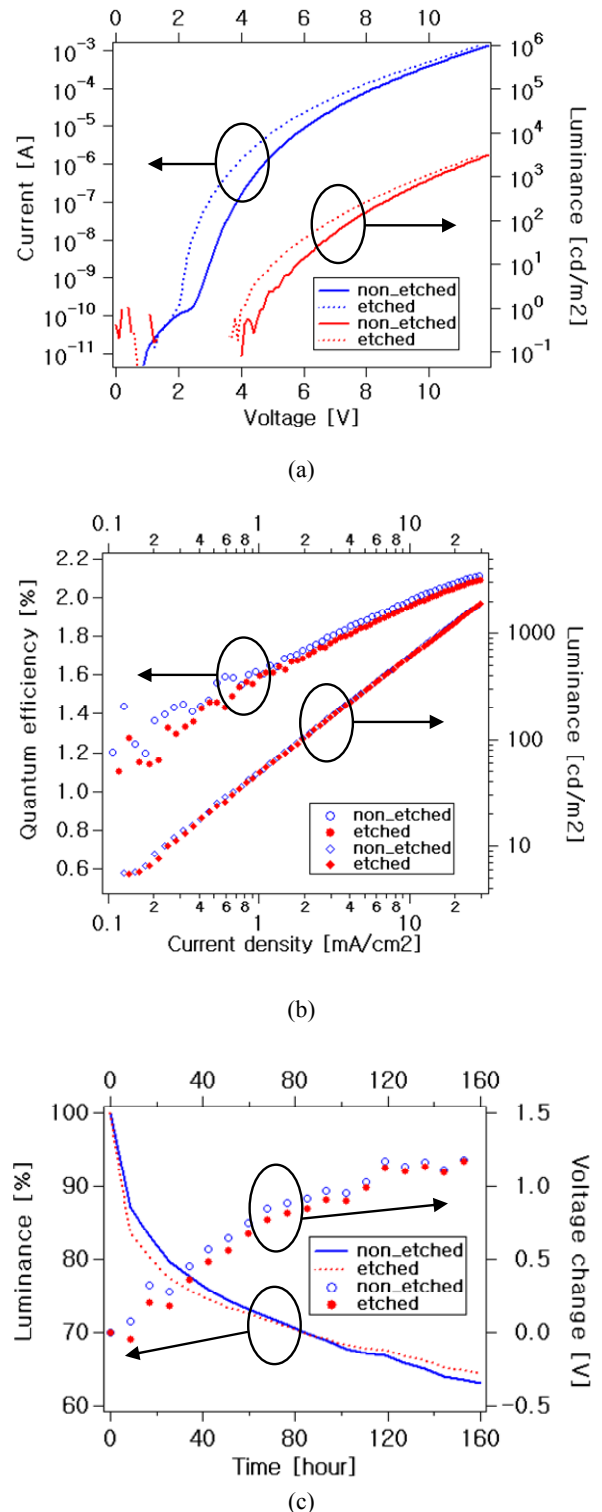


**Fig. 2.** (a) Current and luminance vs. voltage. (b) Luminance and external quantum efficiency vs. current density. (c) Luminance and voltage change with stress time for the etched and non-etched OLEDs. The initial luminance was  $1600\text{cd}/\text{m}^2$  for both the etched and non-etched OLEDs.

150 W RF power levels, for 4 min (c). After the oxygen plasma etching, all the samples were again transferred to the OLED deposition chamber, and then a 100-nm-thick second aluminum cathode was deposited (d). Finally, all the samples were encapsulated with glass caps and UV-curable glue. The whole oxygen plasma etching process, including the transfer processes, took about 15 min.

The actual emitting area was also varied ( $2\times 0.4$ ,  $2\times 0.9$ , and  $2\times 1.4$  mm<sup>2</sup>) to determine if the current increase comes from the leakage current due to the etched edge of the OLED device. Each of the OLEDs with different sizes were denoted as S (small), M (medium), and L (large) for both the etched and non-etched OLEDs, as shown in Fig. 3(a). In addition, the plasma etching time was varied (0, 2, and 4 min) to determine if the hole injection layer causes a current increase when it is exposed to oxygen plasma.

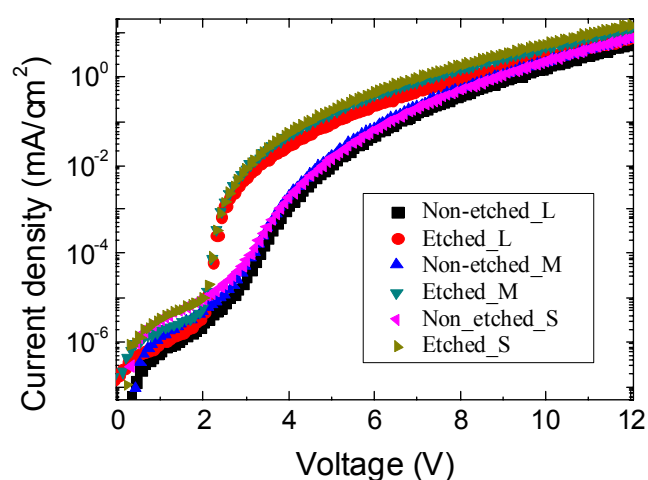
The OLED characteristics were measured using a Keithley 236 voltage/current source, a Keithley 2000 multimeter, and an ARC spectropro-275 monochromator. The external quantum efficiency was extracted from the spectral distribution and luminance measurement data. The lifetime was measured using the McScience MC9600 system, and the changes in voltage and luminance were monitored by applying a constant current. The surface morphology was investigated using the XE-100 atomic-force measurement system. All the measurements were performed in air.

### 3. Result and Discussion

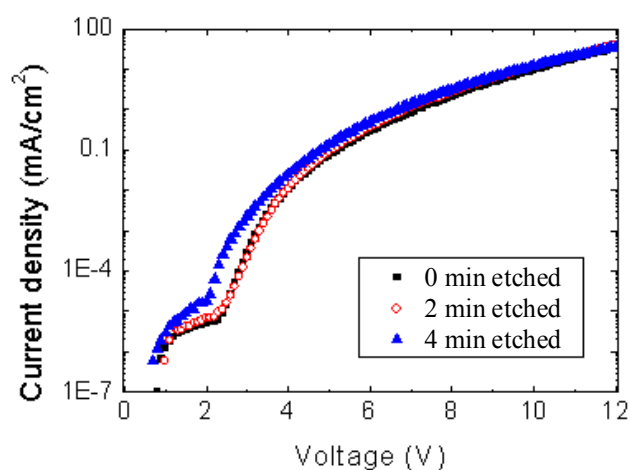
Fig. 2 shows the electrical and optical properties of the fabricated OLEDs. The solid and dotted lines, and the solid and open symbols, represent the measurement data for the non-etched and etched OLEDs, respectively. There were some variations in the current and luminance levels at the same voltage levels. It is believed that these variations are related to the exposure of the devices to air during the transfer process. In fact, some dark spots for the OLEDs exposed to air were observed, which can cause non-uniform device performances [9]. Although air exposure can have different additional effects on the device performances, it is assumed that similar performance changes occurred during the fabrication processes because an attempt was made to minimally and equally expose both devices to air during the whole fabrication process. Based on the experiment, the etched OLEDs commonly showed relatively higher current and luminance levels at the same voltages over low voltage

ranges. As the voltage increased, however, the current and luminance levels started to converge for the etched and non-etched devices. Although it is believed that any defect created at the etched sides of the organic layers can cause an additional current flow for low operation voltages [6], the results showed that the current increase may not come from the defects at the etched sides of the organic layers, which will be discussed later. As the voltage increases, the current flow that actually contributes to light emission increases, becoming a dominant element of the whole device current flow, as shown in Fig. 2(a). It was also commonly observed that the etched devices showed low turn-on voltages of around 2 V while the non-etched devices showed relatively high turn-on voltages of around 3 V. In this case, the turn-on voltages were defined as the voltages where the current flow increases in a stepwise manner for the semi-log current-voltage plots, as shown in Fig. 2(a). Fig. 2(b) shows the luminance and external quantum efficiency vs. current density for the non-etched and etched OLEDs. The external quantum efficiencies of the etched OLEDs are comparable to those of the non-etched devices. It was observed that the performance varied within about 0.2% from batch to batch due to the temperature and humidity variations because the devices had to be exposed to air during the process. In general, however, at the same current densities, the luminance and external quantum efficiencies of the etched and non-etched devices from the same batches were comparable. The lifetime of both OLEDs was measured by applying a constant current to produce the same luminance of 1600 cd/m<sup>2</sup>. The initial voltages and currents at this luminance were 12.8V and 0.7mA and 12.2V and 0.7mA for the etched and non-etched OLEDs, respectively. Fig. 2(c) shows the voltage change and relative luminance progression with the operation time. When the initial luminance reached 70% of the initial luminance, the operation time and voltage increases were 82.4 and 83.6 h and 0.82 and 0.9 volts for the etched and non-etched OLEDs, respectively. It was noted that the plasma-assisted etching process did not greatly affect the OLED performances and lifetime behaviors.

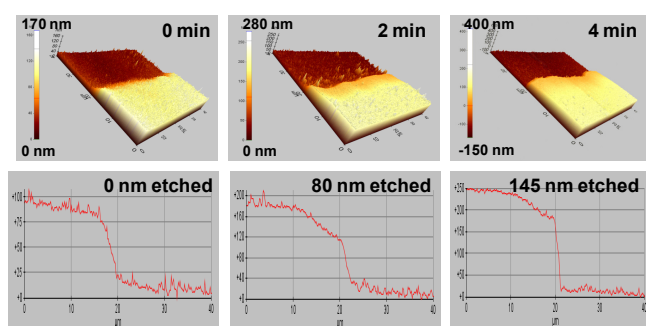
To further investigate the current increase at a low voltage, the current density vs. voltage characteristics of the OLEDs were measured by changing the size of the light-emitting area and the etching time, which expose different layers of the OLED stack to oxygen plasma during the etching process. Fig. 3(a) shows the current density vs. voltage of the non-etched and etched OLEDs with different light-



(a)



(b)



(c)

**Fig. 3.** Current density vs. voltage characteristics of the OLEDs for (a) different light-emitting areas and (b) different etching times. (c) AFM image and step measurement data for different etching times.

emitting areas, which were denoted as S, M, and L at the end of the device name. As mentioned earlier, if the leakage current induced by the defects created at the etched sides is

the main reason for the current increase at low voltages, the OLEDs with different sizes must produce an increase in current density at the same voltage levels, which corresponds to the device size increase. The measurement results that were obtained, however, showed quite similar current density increases for all the three OLEDs, indicating that the current increase at low voltages may not be caused mainly by the leakage current at the etched sides. Fig. 3(b) shows the current density vs. voltage characteristics of the etched OLEDs for different etching times. When the OLEDs were etched for 2 and 4 min, about 80- and 145-nm organic layers were etched. The estimated etching rate was 38 nm/min. The etching depth was measured with the use of an atomic-force microscope (AFM), as shown in Fig. 3(c). It was noted that the total thickness of the organic layers of the OLEDs was about 145 nm. Therefore, after 2-min etching, all the Alq<sub>3</sub> layers and all the parts of the NPB layer were etched; thus, the m-MTDATA layer was not exposed to oxygen plasma. After 4-min etching, all the organic layers were etched; thus, the edge of the m-MTDATA layer was exposed to oxygen plasma and then to air during the measurement. As shown in Fig. 3(b), a similar current increase at low voltages was observed only for the 4-min-etched OLEDs while the 2-min-etched OLEDs showed similar electrical characteristics as those of the 0-min-etched OLEDs. Based on these results, it was speculated that the property of the m-MTDATA layer is more subject to oxygen plasma than the Alq<sub>3</sub> and NPB layers are, leading to a current increase at low voltages, since m-MTDATA is a relatively reactive material under oxygen plasma due to its methyl side chain. It is known that the current increase at low voltages (i.e., the turn-on voltage shift) is closely related with the injection barrier property at the ITO anode and HIL layer and/or HIL and HTL layers, which can be varied via molecular alignment, oxygen content variation of the ITO surface, or interface morphology [11]. Therefore, it is speculated that any chemical reaction of the m-MTDATA layer with oxygen radicals during the etching process may change the effective injection barrier by changing the side chain length, thus thinning the barrier between the conjugated backbone and the metal-organic contact, resulting in the enhancement of the injection current [12], or inducing a molecular-alignment change that causes an interface property change [13], although the molecular-alignment change of the HIL layer is typically obtained from the ultraviolet (UV) or oxygen plasma surface treatment of the ITO sur-

face [10, 13]. Although far-reaching lateral damage to the organic layer from the oxygen plasma, even below the etch mask layer, and the creation of charged states, have been reported for OTFT [6], further analysis is required to investigate the effect of oxygen plasma lateral reaction with the organic layers of the OLED stack because the plasma etching process is typically an anisotropic vertical etching process [5].

#### 4. Conclusion

In this study, it was proposed that the plasma-assisted patterning method can be used to solve the voltage drop along the common electrode of AMOLEDs, and its effects on OLED performances and lifetime were studied to determine the feasibility of the proposed method since it is believed that the plasma etching process can damage the organic layer and can cause performance degradation. Comparable device performances and lifetime were demonstrated for etched and non-etched devices. It was noted that although there was a current increase at low voltages for the etched OLEDs, there were only small changes in external quantum efficiencies and lifetime behavior. The current increase behavior was investigated by changing the device size and etching time. It was found that the leakage current at the etched sides may not play a key role in the current increase, and that m-MTDATA is more subject to chemical reaction under oxygen plasma, leading to a current increase at low voltages by effectively changing the injection barrier. This turn-on voltage shift without a significant change in emission efficiencies can have a positive effect in terms of

the power efficiency of the OLEDs. Therefore, it is believed that the plasma-assisted patterning method can be easily applied to the conventional AMOLED process because one additional shadow mask and oxygen plasma process is needed.

#### Reference

- [ 1 ] G. Gu and S. R. Forrest, *IEEE J. Sel. Topics Quant. Elec.*, **4**, 83 (1998)
- [ 2 ] M. K. Kand and L. J. Guo, *J. Vac. Sci. Tech.* **B 25**, 2637 (2007).
- [ 3 ] C. M. Dunskey, in *Proc. SPIE*, (2005), p. 200.
- [ 4 ] J. Yang, J. Kwak, C. Lee, and Y. Hong, in *Proc. of IMID/Asia Display*, (2008), p. 481.
- [ 5 ] M. Sugawara, *Plasma Etching Fundamentals and Applications* (Oxford University Press, London, 1998) p.66.
- [ 6 ] S. Steudel, K. Myny, S. D. Vusser, J. Genoe, and P. Heremans, *Appl. Phys. Lett.* **89**, 183503 (2006).
- [ 7 ] L. Zhou, A. Wanga, S.-C. Wu, J. Sun, S. Park, and T.N. Jackson, *Appl. Phys. Lett.* **88**, 083502 (2006).
- [ 8 ] N.-B. Choi, D.-W. Kim, H.-S. Seo, C.-D. Kim, H. Kang, M.-J. Kim, and I.-J. Chung, *Jpn. J. Appl. Phys.* **46**, 1333 (2007).
- [ 9 ] M. Fujihira, M. D. Lee, A. Koike, et al., *Appl. Phys. Lett.* **68**, 1787 (1996).
- [ 10 ] Y. W. Park, J. H. Jang, Y. M. Kim, et al., *Thin Solid Film* **10**, 1016 (2009).
- [ 11 ] M. Halik, H. Klauk, U. Zschieschang, G. Schmid, S. Ponomarenko, S. Kirchmeyer, and W. Weber, *Adv. Mater.* **15**, 917 (2003).
- [ 12 ] S. R. Marder, C. B. Gorman, B. G. Tiemann, J.W. Perry, G. Bourhill, and K. Mansour, *Science* **261**, 186 (1993).
- [ 13 ] S. Y. Kim, J. L. Lee, K. B. Kim, and Y.H. Tak, *J. Appl. Phys.* **95**, 2560 (2004).